ISH Journal of Hydraulic Engineering

ISSN: (Print) (Online) Journal homepage: https://www.tandfonline.com/loi/tish20

Bed configurations downstream combined V-Notch-sharped edged Weir with inverted V-Shaped gate

Mohamed M. Ibrahim, Al Sayed Ibrahim Diwedar, Ahmed M. Ibraheem, Noha F. Fathallah & Amir Ibrahim

To cite this article: Mohamed M. Ibrahim, Al Sayed Ibrahim Diwedar, Ahmed M. Ibraheem, Noha F. Fathallah & Amir Ibrahim (05 Dec 2023): Bed configurations downstream combined V-Notch-sharped edged Weir with inverted V-Shaped gate, ISH Journal of Hydraulic Engineering, DOI: 10.1080/09715010.2023.2290102

To link to this article: https://doi.org/10.1080/09715010.2023.2290102

Published online: 05 Dec 2023.

ISH JOURNAL OF HYDRAULIC ENGINEERING
https://doi.org/10.1080/09715010.2023.2290102

Taylor & Francis
Taylor & Francis Group

Bed configurations downstream combined V-Notch-sharped edged Weir with inverted V-Shaped gate

Mohamed M. Ibrahim[a], Al Sayed Ibrahim Diwedar[b], Ahmed M. Ibraheem[b], Noha F. Fathallah[b] and Amir Ibrahim[c]

[a]Shoubra Faculty of Engineering, Benha University, Shoubra, Egypt; [b]National Water Research Center, Hydraulics Research Institute, Shoubra El-Kheima, Egypt; [c]Benha Faculty of Engineering, Benha University, Benha, Egypt

ABSTRACT

Weirs and gates are hydraulic structures installed in canals, mainly for controlling the discharge. Because of their existence, unfavorable influences regarding the downstream bed configurations were recorded. This study experimentally explores the combined effect of simultaneous flow through a hydraulic device consisting of a V-notch sharped weir with an inverted V-shaped gate, aiming to minimize the downstream bed scour. Eighty-one runs were carried out using nine weir-gate models with three different vertex angles. The tests were executed considering three upstream and three downstream water depths. A V-notch weir with an angle of 120° was tested under similar hydraulic conditions and was used for comparison. The results revealed that the length of backflow was increased by the decrease in weir angle under a fixed 120° gate angle. The bed configurations were sensitive to gate angle. The combined device showed a significant decrease in bed disturbances regardless of the angles used compared to the traditional V-notch weir. Simple formulas were developed to predict the scour parameters.

ARTICLE HISTORY
Received 6 June 2023
Accepted 28 November 2023

KEYWORDS
V-Notch Weir; inverted V-Notch gate; compound structures; velocity distribution; scour

1. Introduction

A weir serves as an overflow structure designed for measuring discharge and is typically constructed perpendicular to the axis of an open channel. There are primarily two types of weirs: sharp-crested and broad-crested. Combining a weir with sluice gates can address some of their individual limitations. Sluice gates tend to retain floating objects, a concern that can be mitigated when used alongside weirs. Downstream of hydraulic structures, the flow pattern manifests as jets, contributing significantly to scouring. Researchers often initiate studies to examine scour depth (ds) and scour length (Ls). Local scour remains a persistent subject of investigation, with numerous researchers contributing to the field (e.g., Basiouny et al. 2018a; Helal 2014; Dey and Barbhuiya 2005; Zhang et al. 2009; Sheppard et al. 2013; Ibrahim et al. 2018; Basiouny et al. 2018b; Abdelhaleem and S 2023). Furthermore, weirs create stagnant water areas upstream, where sediment accumulation can disrupt flow conditions. Combining a weir with a gate is a practical solution in such scenarios. Ibrahim (2015) conducted experimental evaluations on a compounded V-notch weir with double triangular pieces and various notch angles, proposing it as an alternative to the traditional V-notch weir. Additionally, an empirical equation (Eq. 1) was derived to predict relative scour depth.

$$\frac{d_s}{y_t} = 0.273\frac{h}{y_t} + 7.423\frac{d_{50}}{y_t} + 0.968F_r - 0.0021\theta_w + 0.448 \quad (1)$$

In which: scour depth (d_s); head of water over weir (h); tailwater depth (y_t); tail Froude's number (Fr); the angle of V-notch weir (θ_w); median particle diameter (d_{50}).

Hamed et al. (2009) explored the physical impact of V-notch and oblique weir angles on bed topography; they found that constructing a V-notch weir with a small oblique angle can reduce scour parameters. Notably, V-notch angles of 30°, 60°, and 90° had minimal effects, while 120° had a significant positive impact. Dehghani et al. (2010) conducted a physical model study of compound system weirs with gates and observed an inverse relationship between relative maximum scour depth, relative gate opening, and relative head over the weir. Flow over weirs was identified as the primary cause of scour. Omran et al. (2016) investigated the influence of combined structures, such as weirs and gates, on scour hole characteristics. Rectangular and triangular gates were found to be more effective than circular gates in reducing maximum scour depth. Googheri et al. (2017) utilized FLOW-3D to study composite weir-gate effects on bed configuration, revealing a 38% decrease in energy dissipation. Elkiki (2018) assessed scour parameters downstream of skew V-notch weirs, finding that using the Gene Expression Programme (GEP) model was more effective than Artificial Neural Network (ANN) and Multiple Linear Regression (MLR) Modelling. El-Mahdy (2021) examined V-notch end sills' impact on energy dissipation and bed configurations, showing improved energy dissipation with lower angles. Abdulabbas et al. (2015) studied compound structures of weirs and gates, with trapezoidal upper and triangular lower parts resulting in the minimum values. Namadian and Asadi (2022) investigated scour depth downstream of combined weir-gate systems, noting a decrease with increased valve opening. Ogden et al. (2011) evaluated sedimentation's impact on a 140° V-notch weir's discharge coefficient, finding a direct proportionality.

Saadatnejadgharahassanlou et al. (2019) simulated flow over a sharp-crested V-notch weir, favoring a Reynolds stress model (RSM) for flow characteristics prediction. Rezazadeh et al. (2020) used Open FOAM to analyze sharp-crested

CONTACT Amir Ibrahim Amir.ibrahim@bhit.bu.edu.eg

weirs, finding the greatest discharge coefficient for rectangular weirs. Tanimu et al. (2021) studied trapezoidal weirs combined with semi-circular gates, revealing an increased discharge coefficient compared to block weirs. Latifi et al. (2018) investigated scour parameters downstream of single and combined jets, indicating a positive impact of combined jets on reducing scour. Mohamed and Abdelhaleem (2020) explored sluice gates with orifices, finding them effective in dissipating jump energy and reducing local scour. Abozeid et al. (2019) studied broad-crested weirs with orifices, observing reduced scour characteristics and apron length with bottom openings. Saad and Fattouh (2016) preferred three openings in broad-crested weirs for reducing near-bed velocity and hydraulic jump length. Daneshfaraz et al. (2019) used a 3D numerical model to analyze broad-crested weirs with orifices, noting boosted discharge coefficients and lower water levels. Alhealy and Hayawi (2019) confirmed the effectiveness of weirs with holes in decreasing downstream scour.

In open channels, the triangular V-notch weir is an accurate measurement tool, but a compound V-notch weir with two pieces may release high discharge with good accuracy, which leads to increased local scour downstream this type of weir. There is minimal data on the scour downstream of the combined V-notch weir, and the majority of previous research focused on the discharge coefficient of flow passed through these combined structures. Therefore, the main objective of this experimental study was to evaluate the local scour downstream of a combined V-notch sharped weir with an inverted V-shaped gate with different angles and compare these values under the same flow conditions.

2. Experimental setup and procedures

2.1. Experimental setup

The experimental study was implemented in the hydraulic laboratory at the Hydraulics Research Institute (HRI), National Water Research Center (NWRC), Egypt. A 3-D flume model was used to study the influence of the combined structure of a V-notch weir with an inverted triangular V-notch gate. The flume is 23 m long, 1.4 m wide and 0.6 m deep. The bottom floor of the flume model is made of concrete and the side walls are made of bricks that are covered by mortar to prevent leakage. The tailwater depth is controlled by a tailgate fixed at the flume end. The flume is fed with water from a head tank. The centrifugal pump with a total discharge of 150 L/s conveys the water from the sump to a reservoir, where the flow passes through the flume. The flume inlet consists of a masonry basin of 3.80 m length, 1.7 m width and 2.5 m depth. The flow passes through a screen box filled with large gravel that is fixed to the stilling basin.

The stilling basin has a length of 5.0 m and starts 12.5 m downstream of the flume inlet. The basin length is divided into three parts; 1.0 m upstream of the gravel box, 2.0 m between the gravel box and the composite V-notch weir-gate, and 2.0 m, which is the apron length located downstream of the compound structure. This length achieves the appropriate distance for the movable bed from the zone of water turbulence, see Figure 1.

The stilling basin is followed by 4.0 m of a movable bed material of median particle diameter; $d_{50} = 0.432$ mm (medium sand-depending on US Bureau of Soil Classification; Trishan 2020), $d_{90} = 0.664$ mm, and geometric standard deviation $\sigma_g = 1.413$ to represent the bed sediment, dry bed material angle of repose equal to 29°, and specific gravity of bed material, $S_g = 2.60$, The tested bed material was uniform according to (Dey et al. 2008; Shan et al. 2012). The depth of the movable bed material is 0.30 m.

The utilized composite weir-gate structure is made of steel 0.5 m high, 1.40 m wide, and 0.002 m thick. The upper edge of the used weir formed a V-notch sharp crested weir, and the bottom edge formed an inverted V-notch shaped gate. The height of the gate d = 0.175 m, the height between the upper edge of the triangular gate and the bottom edge of the V-notch weir y = 0.15 m, and the height of V-notch weir W = 0.175 m. For comparison purposes, the previous weir dimensions are kept constant for all tested models.

2.2. Experimental program

Head of water over weir h, tail water depth, angle of the V-notch sharp weir, and angle of the inverted triangular gate, selected independent variables were the focus of the test program. Nine tests were conducted for each composite model, as shown in Table 1. There were three inverted gate angles and three weir angles evaluated. Three water depths above the weir (h = 0.10, 0.13, and 0.16 m) and three tail water depths ($y_t = 0.20$, 0.225, and 0.25 m) were studied for each angle. Used a digital point gauge with an accuracy of ±0.1 mm, the water level in the weir-gate model was measured both upstream and downstream, velocity was measured by using an Electromagnetic Current-meter type E.M.S. with a 0.2% accuracy. Eighty-one experimental by using nine different weir models were executed, as shown in Figure 2.

2.3. Experimental procedures

The tailgate was completely closed, and the downstream feeding gradually started until its depth became higher than the tailwater depth. This was done after the weir model was fixed in the desired location on the apron and the flume was filled with bed material and precisely levelled at its place in the model using a levelling device. The main pump was turned on simultaneously until it reached the intended head over the V-notch weir. The appropriate tail water depth was adjusted by gently tilting the tailboard. Consequently, the run time duration was begun; according to Melville and Chiew (1999), the equilibrium time for scour depth is the period of time during which the depth of the scour does not fluctuate by more than 5% of the obstruction's width. Initial tests showed that 22 h were sufficient to reach this condition. Six hours were used as the duration for comparison's sake. The pump was switched off and the test run was stopped. The flume was drained gradually at a slow rate to keep the bed material in place with no movement. The bed configuration was recorded using levelling device at various locations of the designed mesh, each 0.10 m in the x-direction and 0.25 m in the y-direction. All previous steps were repeated for each run.

3. Dimensional analysis

Variables affected the bed configurations downstream of V-notched weir – gate can be expressed in the following functional form:

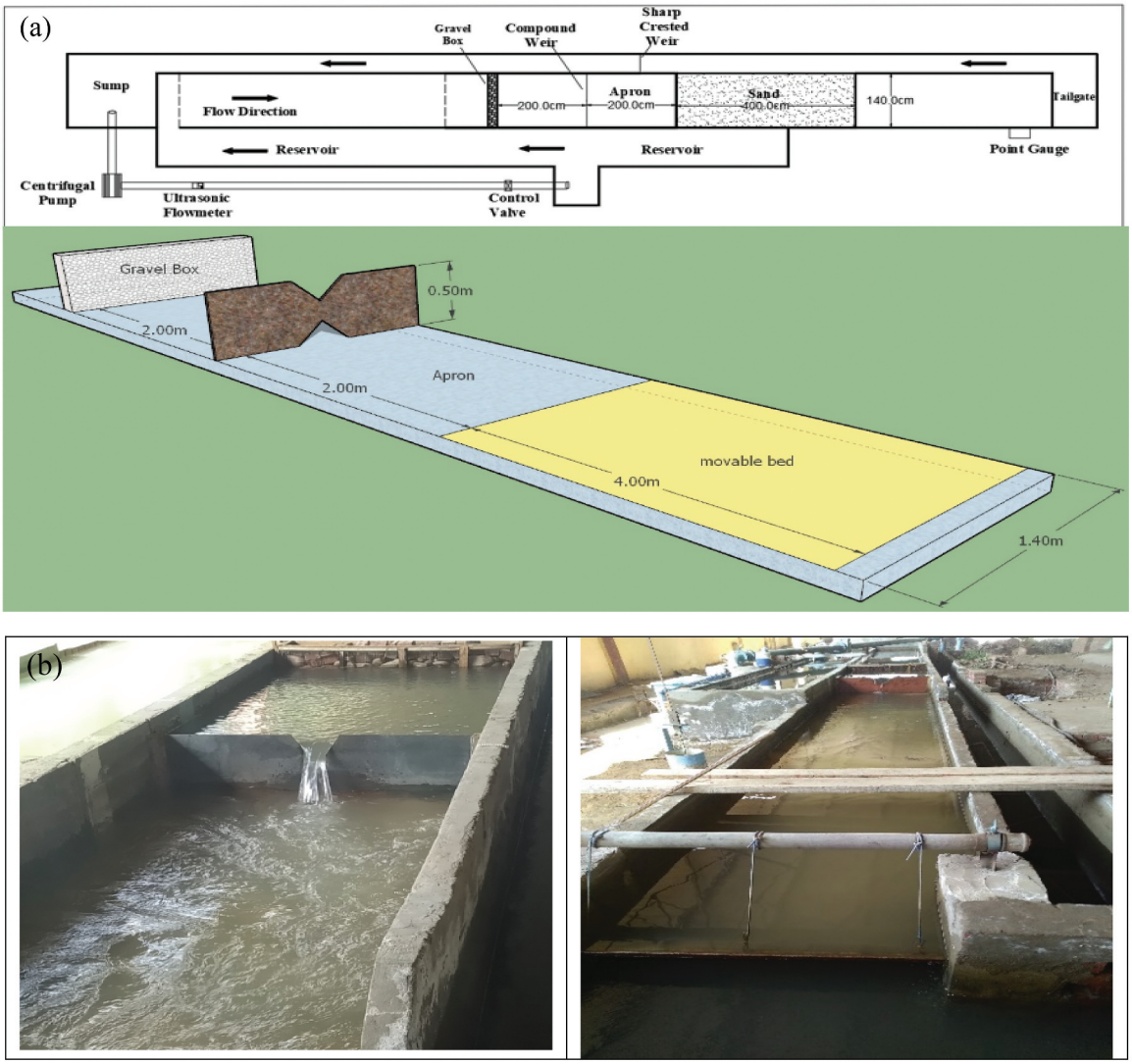

Figure 1. a) flume layout b) flume in the laboratory.

Table 1. Experimental tested flow conditions.

Model No.	Angle of V-notch weir θ_w (°)	Angle of inverted V-notch gate θ_g (°)	Head of water over the weir h (m)	Tailwater depth y_t (m)
1	60	60	0.10,0.13,0.16	0.20,0.225,0.25
2	60	90		
3	60	120		
4	90	60		
5	90	90		
6	90	120		
7	120	60		
8	120	90		
9	120	120		

$$f\left(d_s, L_s, X, B, d, y, h, y_t, b_1, g, \theta_w, \theta_g, S_o, L_{ap}, Q, L, d_{50}, \rho, \mu\right) \tag{2}$$

In which: flume width (B); height of the gate (d); the discharge (Q); tailwater depth (y_t); distance between bottom edge of V-notch weir and upper edge of the inverted triangular V-notch gate (y); bottom width of the inverted V-notch angle (b_1); the longitudinal distance downstream of apron length (X); scour depth (d_s); head of water over weir (h); scour length (L_s); angle of the triangular V-notch weir (θ_w); gravitational acceleration (g); angle of the inverted triangular V-notch gate (θ_g); bed slope (S_o); apron length (L_{ap}); movable bed length (L); water density (ρ); dynamic viscosity (μ), study parameters are shown in Figure 3. The following dimensionless groups can be derived to represent the phenomenon based on dimensional analysis using Buckingham's theorem:

$$f\left(\frac{d_s}{y_t}, \frac{L_s}{y_t}, \frac{X}{L}, \frac{d_{50}}{y_t}, \frac{d}{y_t}, \frac{Q*\rho}{B*\mu} = R_e, \frac{y}{y_t}, S_o, \frac{b_1}{y_t}, \frac{y}{y_t}, \frac{Q^2}{g*B^2*y_t^3} = F_r^2 = \lambda, \frac{\theta\ \mathrm{w}}{\theta\ \mathrm{g}}, \frac{\mathrm{B}}{y_t}\right) = 0 \tag{3}$$

In which Froude's number (F_r); kinetic flow factor (λ); Reynolds' number (R_e), in this study, y, g, S_o, L_{ap}, d_{50}, ρ, and μ, are maintained constant, thus Equation (4) does not include them.

$$f\left(\frac{d_s}{y_t}, \frac{L_s}{y_t}, \frac{X}{L}, \frac{d}{y_t}, \frac{b_1}{y_t}, \frac{y}{y_t}, F_r^2 = \lambda, \frac{\theta\ \mathrm{w}}{\theta\ \mathrm{g}}, \frac{\mathrm{B}}{y_t}\right) = 0 \tag{4}$$

4. Results and discussions

The eight subsections that follow discuss the laboratory work's findings in relation to the four investigated parameters. The statical determination for constants proposed

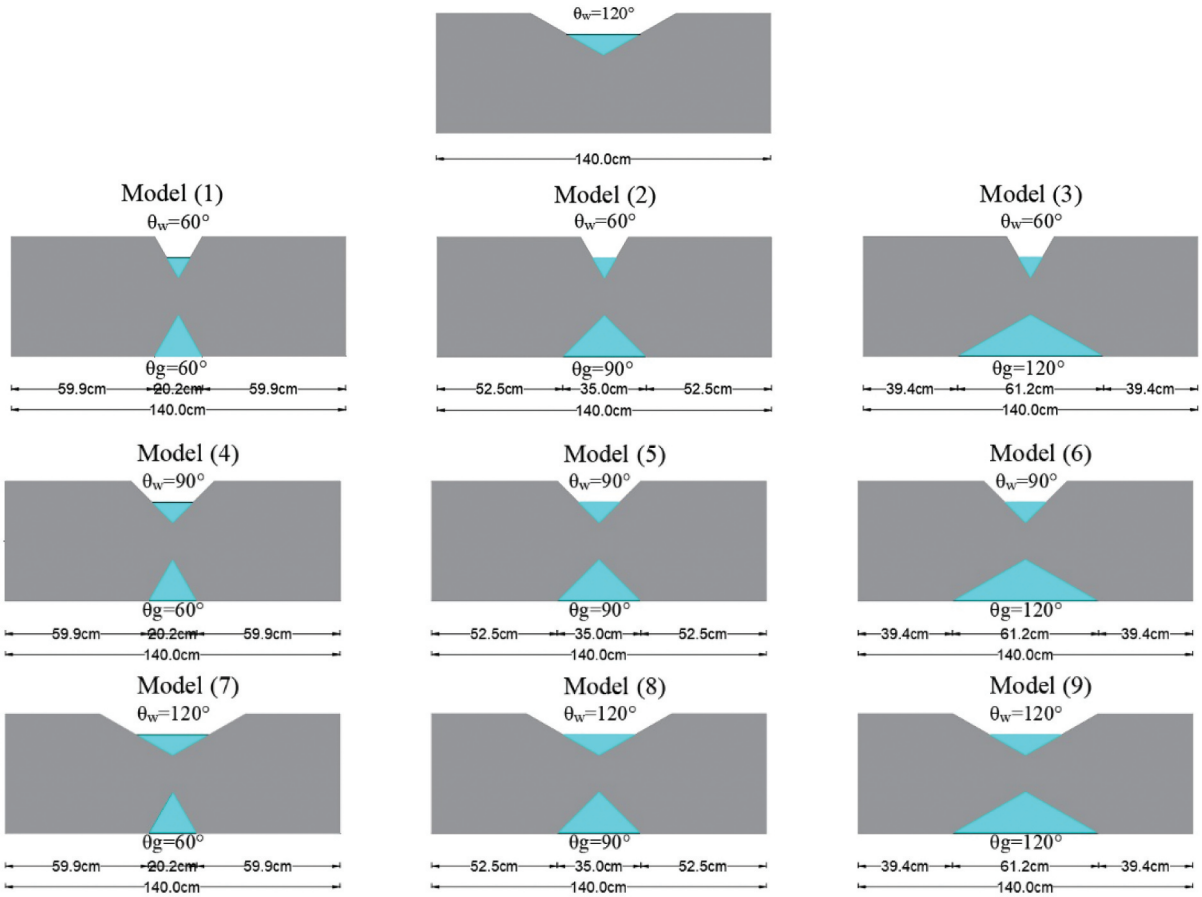

Figure 2. Details of the tested Weir scenarios with different angles.

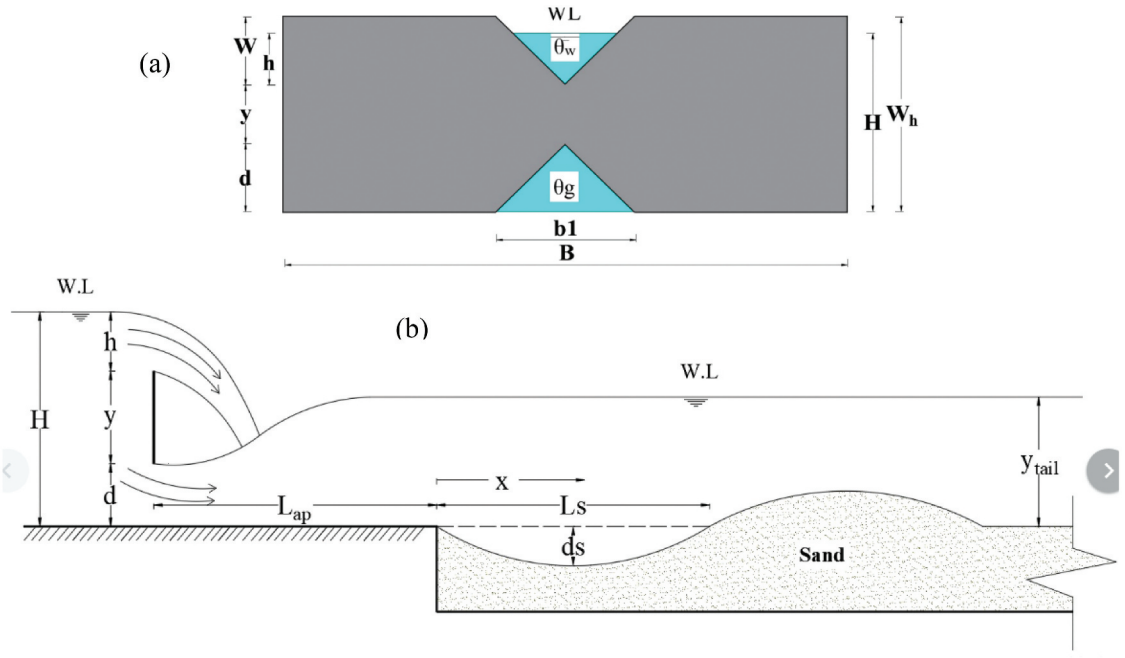

Figure 3. Study parameters a) definition sketch of the tested weir b) definition longitudinal section.

by dimensional analysis for the scour depth and length formulas is illustrated in the ninth subsection.

4.1. The velocity distribution downstream of the weir apron

The flow path was followed for 4.0 m along nine profiles, starting from the end of the weir apron and extending to the end of the movable bed area, to estimate the velocity at the centre line. Each profile was set apart by a fixed distance of 0.5 m. The vertical velocities at each profile were measured at 0.2, 0.4, 0.6, 0.8, and 0.9 of the reported tailwater flow depths, y_t. Figure 4 illustrates the influence of gate angle on the velocity distribution downstream of the weir apron for the flow condition of the highest head over the weir and the least tailwater depth (h = 16 cm, y_t = 20 cm). The figure shows that changing

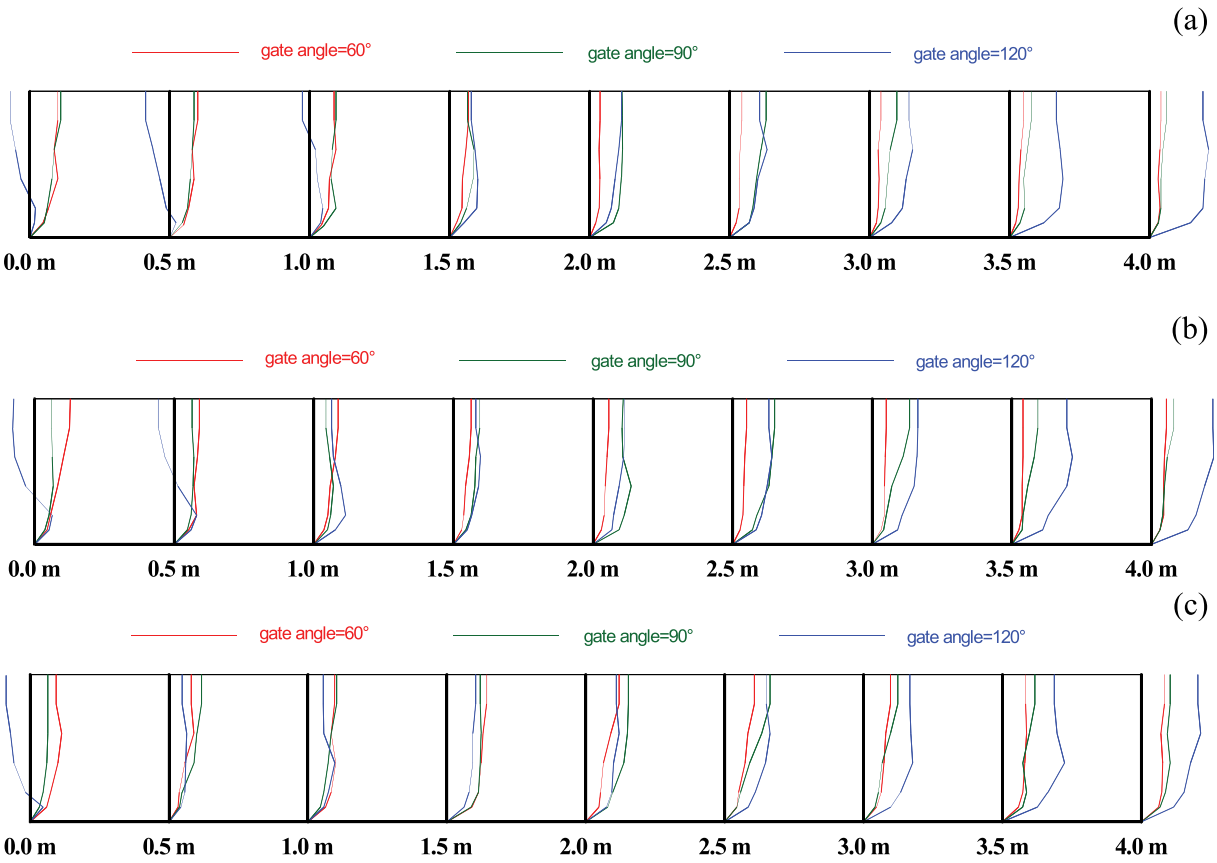

Figure 4. Velocity distribution from h = 16cm and y_t=20cm, a) θw = 60°, (b) θw = 90°, and (c) θw = 120°.

the gate angle with a constant weir angle has a great effect on increasing the velocity measured because the gate angle is responsible for passing the large ratio of the flow discharge compared to the weir angle. In addition, increasing the gate angle from 60° to 90° has no remarkable impact on increasing or changing the flow behavior in contrast increasing the gate angle to 120° extremely increases the velocity and generates a zone of reverse flow with different weir angles of (θw = 60 °, 90 °, and 120 °). The length of reverse flow is inversely proportional to the weir angle; that caused by the flow passing through small weir angles is not enough to dissipate the energy due to the flow under a gate of angle 120°.

4.2. Effect of Weir angle on scour parameters

Figure 5(a) investigates the effect of the weir angle (θ_w) on changes in the bed configuration. The presented figure is plotted for bed changes at the center line for gate angle 90 ° with different modes of weir angle (θ_w = 60°, 90°, and 120°) for flow condition of (h = 16 cm and y_t = 20 cm). The figure illustrates that relative scour depth increases with the increase of the weir angle. The maximum scour depth was recorded at θw = 120° with 44.7% increase compared to θw = 60°. The scour length is approximately the same for different weir angles which forms ratio of 25% of the movable bed length. The figure featured that the deposition height was observed at the same case of scour depth with an increase ratio 51.85% compared to θw = 60°, and the deposition length represents 56.0% of the movable bed length.

4.3. Effect of gate angle on scour parameters

Figure 5(b) shows the bed profile at the flume model's centerline along the movable bed area for different gate angles (θg = 60°, 90°, and 120°) and constant weir angles (θw = 90°). A change in gate angle is particularly effective in bed topography, as shown in Figure 5(b) which is displayed for (h = 16 cm and y_t = 20 cm). The gate angle is directly proportional to the length and depth of the scour. The maximum scour depth increases for gate angles 90 °, and 120 ° by 40% and 360%, respectively, in comparing to maximum scour depth of gate angle 60 °. Additionally, the relative maximum scour length increased by 95% and 194% at gate angles of 90° and 120° compared to 60°. The large increase in maximum scour depth and length is explained by the large increase in discharge passes through the inverted V-notch gate, as discussed in section 4.1.

In Figure 4, the zone of scour started from 2 m downstream of the weir the velocity under θg = 90° approaches the velocity under θg = 120°, because this zone is the beginning of the movable bed. As a result of a greater discharge passing through the angle of 120 °, the scour is highest as shown in Figure 5, which increases the depth of the water and reduces the velocity, but the angle of 90° is allows the passage of a lower discharge and causes less scour and thus a lower water depth, which increases the velocity, which led to a convergence. The velocities in that zone, and explanatory evidence, shown the increase in velocities at angle 120° after the scour zone compared to the angle 90° velocities.

4.4. Effect of head over Weir on scour parameters

Figure 6(a) shows the influence of head over the weir; (h) on the movable bed profile downstream the apron toe of a combined weir structure of 90° V-notch angle with inverted V-notch gate angle of 90°, and tail water depth of 20 cm. It has been clearly observed that an increase in head above the weir causes an increase in the flow passing through

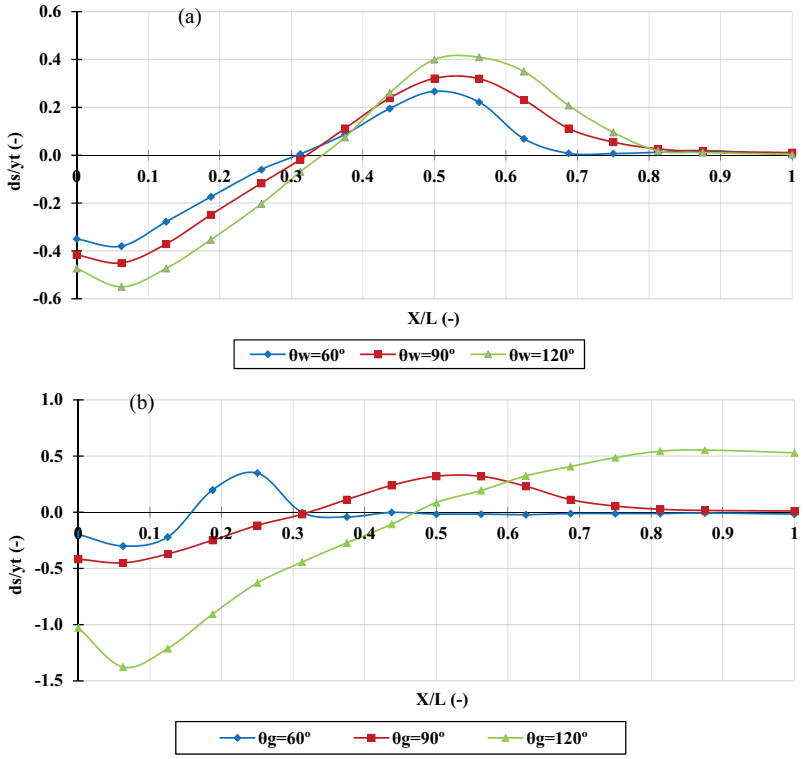

Figure 5. a) Effect of Weir angle on dimensionless maximum scour depth, (ds/y_t), b) Effect of gate angle on dimensionless maximum scour depth, (ds/y_t).

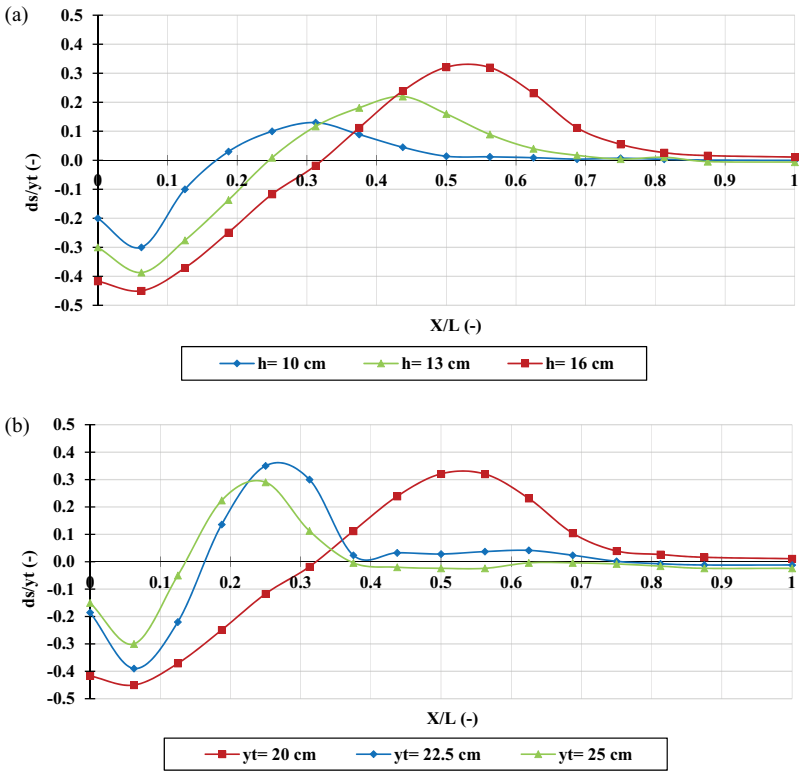

Figure 6. a) Effect of head over the Weir on dimensionless maximum scour depth, (ds/y_t), b) Effect of tail water depth on dimensionless maximum scour depth, (ds/y_t).

the compound weir and thus leads to an increase in relative scour parameters. The relative maximum scour depth for (h = 13 cm and 16 cm) compared to the case of h = 10 cm increased by 33% and 50%, respectively. Also, the relative maximum scour length for (h = 13 cm and 16 cm) with reference to the case of 10 cm increased by 41% and 74%, respectively. The location of maximum scour depth does not change with different conditions of head over the weir. The deposition height and location increase with the increase in head over the weir.at which, the maximum deposition height increased by 75% and 166% for head over weir 13 cm and 16 cm respectively compared to h = 10 cm.

4.5. Effect of tailwater depth on scour parameters

Figure 6(b) shows the influence of the tailwater depth (y_t) on the movable bed profile downstream the apron toe of the combined weir structure of weir angle = 90°, gate angle = 90°, and head over the weir = 16 cm. The figure illustrates that scour parameters are inversely proportional to tailwater depth. The relative maximum scour depth for (y_t = 22.5 cm and 25 cm) in relation to the case of y_t = 20 cm decreased by 12% and 33%, respectively. Also, the relative maximum scour length for (yt = 22.5 cm and 25 cm) compared to the case of 20 cm decreased by 44% and 55%, respectively. The location of the maximum scour depth is almost the same for the different tailwater depths.

4.6. Effect of weir/gate angles on relative maximum scour depth

Figure 7 presents the relative maximum scour depth for different modes of weir angle, gate angle, tail water depths, and constant head over the weir of 16 cm. Figure 7 illustrated the same findings of the previous section. The relative maximum scour depth is almost the same for all modes except modes with gate angle 120°, at which the decrease in relative tail water depth (y_t/h) increases the relative maximum scour depth by 46.67% and 135.38% compared to relative tailwater depth equals 1.56 for θw/θg = 120°/120°. Comparing maximum scour depth with different tailwater depths for the case of weir/gate angles 120°/120° to 60°/60° demonstrated an increase by 469.01%, 263.56% and 225.00% corresponding to relative tailwater depths of 1.25, 1.4 and 1.56, respectively.

The comparison between the minimum and maximum discharge related to the weir and gate angles is shown in Figure 8. The contour map and 3D development of the scour hole for the case of weir/gate angle (60°/60° and 120°/120°) are shown in Figure 8(a–d) for flow condition (h = 16 cm and y_t = 20 cm).

Figure 8(a, b) shows that the scour depth measured in the case of weir/gate angle 60°/60° is 13 cm and reaches to 85.0 cm from the apron toe, and the silting height is 7.0 cm with a length of 65.0 cm.

Figure 8(c, d) illustrates that scour depth observed in the case of weir/gate angle 120°/120° is 26.0 cm which increased

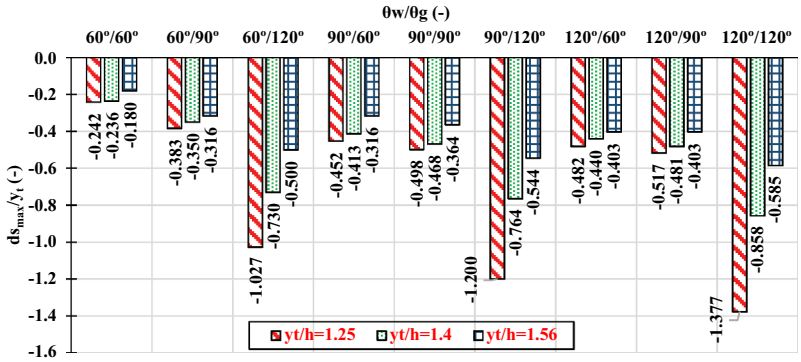

Figure 7. Relation between weir/gate angle and maximum scour depth ds_{max}/y_t.

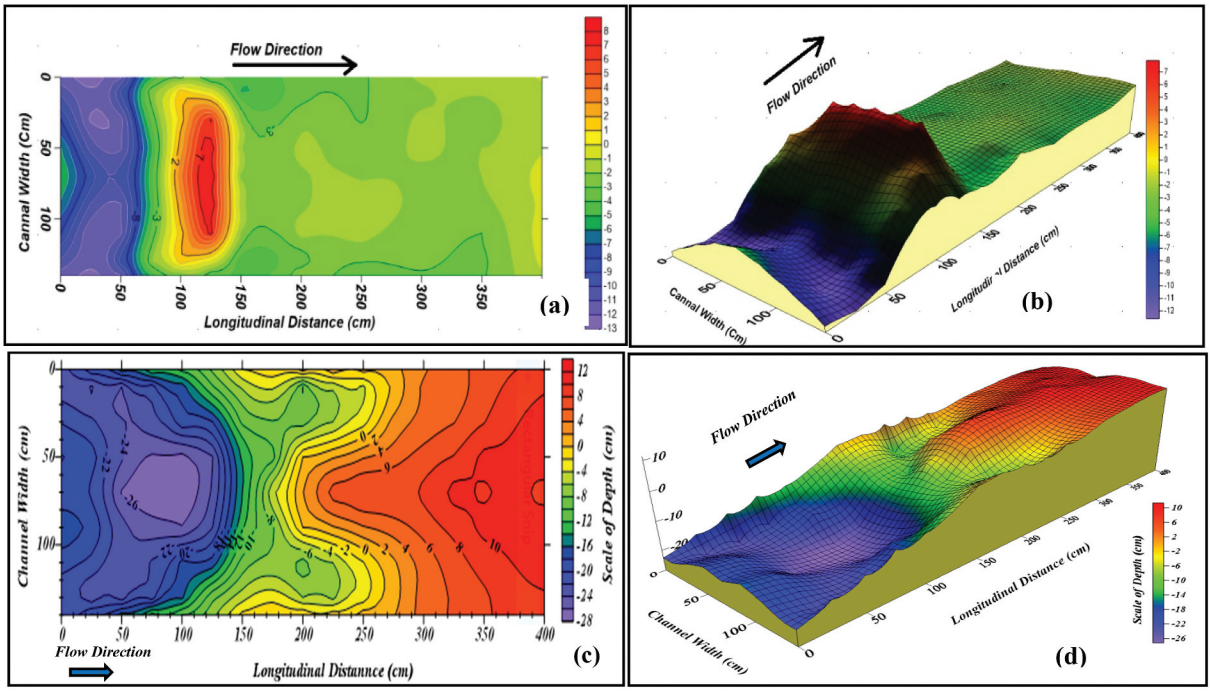

Figure 8. Bed configuration downstream apron for (a, b) θ_w = 60°, θ_g = 60°, h=16cm and y_t = 20cm (a) contour map for scour, (b) 3D development of scour hole, (c, d) θ_w = 120°, θ_g = 120°, h=16cm and y_t = 20cm (c) contour map for scour, (d) 3D development of scour hole.

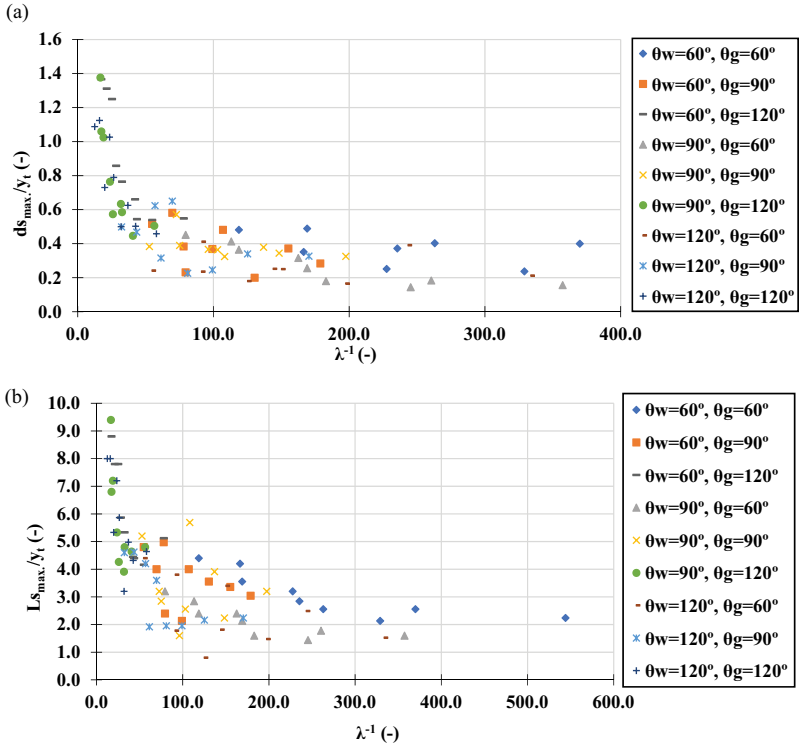

Figure 9. a) relation between $ds_{max.}/yt$ and λ^{-1} for all tested models, b) relation between $Ls_{max.}/yt$ and λ^{-1} for all tested models.

by 100% compared to the angle of 60°/60° with length of scour about 200.0 cm that means increase by 233.33%. The silting height increased by 71.43% and its length reached to the end of movable bed length which is 4.0 m.

4.7. Effect of kinetic flow factor on scour hole parameters

Figure 9(a) presents the correlation between dimensionless maximum scour depth and kinetic flow factor ($Fr^{-2}=\lambda^{-1}$). It is obvious from the presented figure that the maximum scour depth decreases with an increase of λ^{-1}. The relation between the relative maximum scour length and the kinetic flow factor is illustrated in Figure 9(b). It shows that the relation between $Ls_{max.}/y_t$ and λ^{-1} is inversely proportional. The kinetic flow factor was calculated for the tail Froude number located at the end of the flume model and the velocity used was the mean velocity.

4.8. Relative volumes of scour and deposition

Figure 10 presents relative volumes of scour and deposition; V_f/V_t (volume of formation/total volume of movable bed matrial) in Measurement zone along of movable bed for different values of weir and gate angles for the flow condition (h = 16 cm and yt = 16 cm). It is obvious that scour volume increases with increase of gate angle specialy with (θg = 120°) because it passes large amount of flow discharge compared to the flow passed over the weir. The maximum scour volume was observed at (θw/θg = 60°/120°) and it was found to decrease with the increase of weir angle as shown for the case of (θw/θg = 120°/120°). At which, the minimum value of scour volume was observed at (θw/θg = 90°/60°). Also, the figure shows that decreasing the weir angle to 60° makes the flow over the weir not enough to dissipate the energy of flow passes through the gate angle and increasing the weir angle to 120° has negative impact on scour volume because the flow over weir is not enough for a better to dissipate energy.

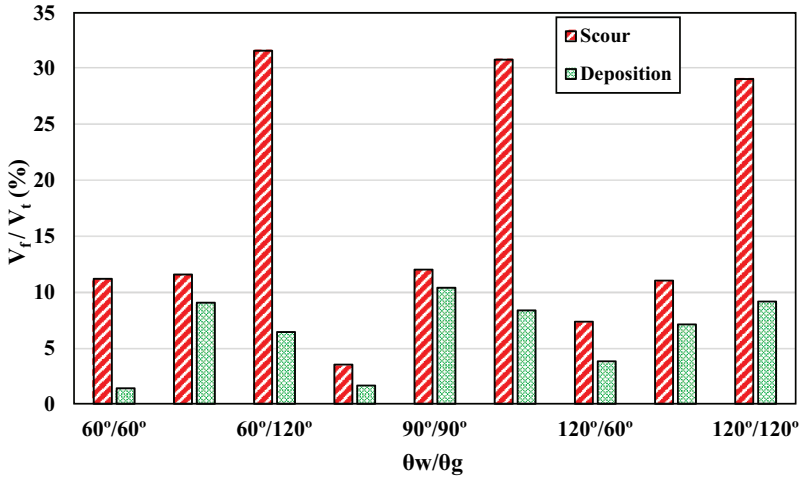

Figure 10. Relative volumes of scour and deposition along of movable bed.

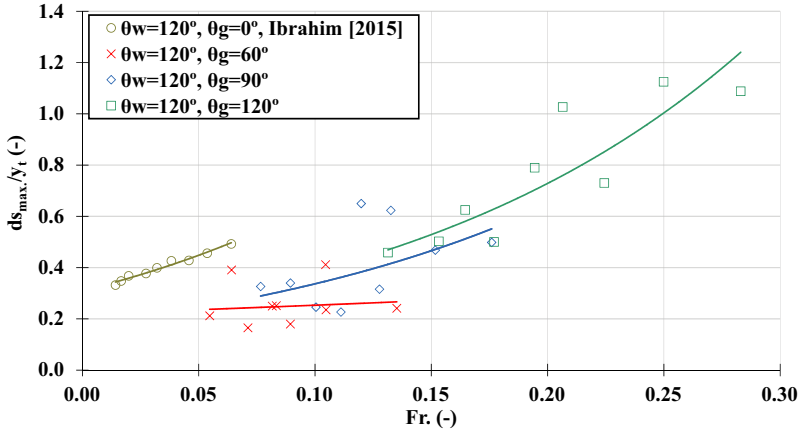

Figure 11. Effect of gate angle (θg) on relative maximum scour depth.

Figure 11 discusses the effect of gate angle (θ_g) on the relative maximum scour depth. The figure presents the higher weir angle (θ_w) of 120° with different gate angles (θ_g) of 0°, 60°, 90°, and 120°. The results of the measured scour depth of the compound weir were compared to calculated data of V-notch weir, from Equation 1, Ibrahim (2015). The figure shows a good correlation between dimensionless maximum scour depth downstream V-notch weir and compound weir at which depth of scour increases with the increase of gate angles, which leads to an increase the discharge and thus an increase in the Froude's number.

The comparison showed that the measured results fell within the predicted range of values. The variation in Froude number caused by the gate angle increasing, which raises the flow discharge beneath the inverted V-notch weir. Discharges passed from 7.8 L/s to 25.1 L/s at (θw = 120°, θg = 0°), ranged from 27.5 L/s to 50.1 L/s at (θw = 120°, θg = 60°), ranged between 41.84 L/s and 68.6 L/s at (θw = 120°, θg = 90°), and ranged between 67.3 L/s and 101.1 L/s for (θw = 120°, θg = 120°). Despite the difference discharges between gate angles 60° and 90°, there is a slight difference in the scour values between them at small discharges for each of them. On the contrary, angle 120° gives high scour values compared to the other angles, exceeding double at many discharges.

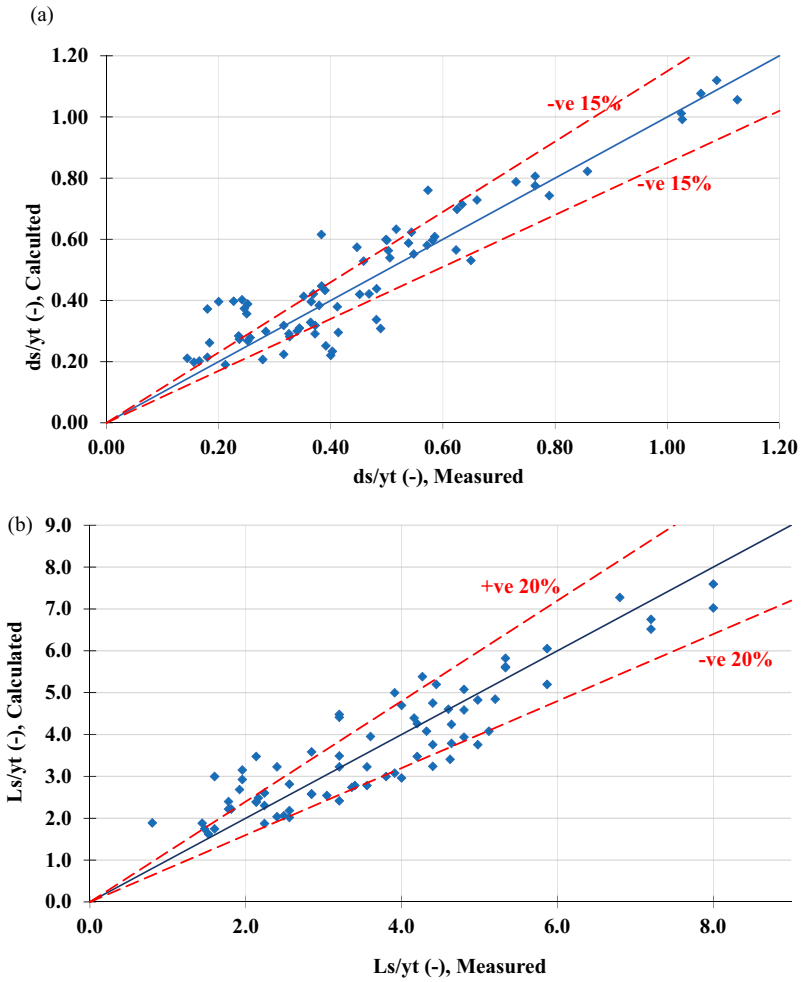

Figure 12. Comparison between measured and calculated values of; (a) relative maximum scour depth; (b) relative maximum scour length.

Table 2. Coefficient values of relative maximum scour depth and Length.

Constants No.	a	b	c	d	e	f	g	R^2
Equation 5	−0.0848	1456.788	$-594*10^{11}$	3.212	$-16*10^{7}$	$5.6*10^{7}$	$207*10^{11}$	0.859
Equation 6	−0.146	1253.688	$-553*10^{11}$	2.392	$40.3*10^{7}$	$-14.1*10^{7}$	$193*10^{11}$	0.821

4.9. Developing empirical equations

Regression analysis models with various dimensionless variables were used to predict empirical equations from experimental data, evaluating relative maximum scour depth and length downstream the compound structure of weir/gate angle. It was found that the dimensionless parameters (θ_w/θ_g, d_{50}/y_t, d/w_h, b_1/B, h/w_h, and h/w) show significant association, table 2 shows the coefficient values of relative maximum scour depth and Length, the obtained formulas can be stated as follows:

$$\frac{ds_{max.}}{y_t} = Exp\left(a\frac{\theta_w}{\theta_g} + b\frac{d_{50}}{y_t} + c\frac{d}{w_h} + d\frac{b_1}{B} + e\frac{h}{w_h} + f\frac{h}{W} + g\right) \quad (5)$$

$$\frac{Ls_{max.}}{y_t} = Exp\left(a\frac{\theta_w}{\theta_g} + b\frac{d_{50}}{y_t} + c\frac{d}{w_h} + d\frac{b_1}{B} + e\frac{h}{w_h} + f\frac{h}{W} + g\right) \quad (6)$$

The developed formulas for relative maximum scour depth and length were validated using measured and calculated values as shown in Figure 12, demonstrated that the experimental values have a good agreement with the predicted values.

5. Conclusions

In the current study, an experimental model was taken into consideration to evaluate the impact of using a combined structure in which the flow passes over a sharp-crest weir with a V-notch and through an inverted V-notch gate on the parameters of the scour hole downstream of the weir apron and the flow velocity distribution in both longitudinal and vertical directions. Eighty-one test runs were carried out, which were divided into 9 weir models. Nine weir models were applied with different angles for both weir and gate. Three different angles were utilized (60°, 90° and 120°) for the weir notch and the inverted gate notch. A classic V-notch weir with an angle of 120° was used to assess the efficiency of utilizing a compound V-notch weir gate. Based on the measured data and analysis, it is concluded that:

- The combined weir, which consists of a V-notch and an inverted V-gate, enables accurate and continuous measurement of various flows, in good accord with (Martínez et al. 2005; Ali et al. 2015).
- Backwater occurs in the case of $\theta_g = 120°$ with different weir angles, its length is inversely proportional to the weir angle.
- An increase in the gate angle with a constant weir angle has a great effect on increasing the vertical velocity measured downstream compound weir because the gate angle is responsible for passing the large ratio of the flow discharge compared to the weir angle.
- The depth of scour increases with the increase of weir and gate angles.
- The length and depth of the scour are inversely proportional to tailwater depth and directly proportional to head over weir.
- Gate angle is the primary factor influencing the scour depth.
- Some experimental equations were presented by using regression analysis to express the relationships between both the relative maximum scour depth and length downstream the compound structure of weir/gate angle and dimensionless parameters (θ_w/θ_g, d_{50}/y_t, d/w_h, b_1/B, h/w_h, and h/w), the deduced equations are applied within the limits of this study.

Acknowledgements

This experiment was implemented at Hydraulics Research Institute, National Water Research Center (NWRC), Egypt. The authors gratefully thank the institution for collaboration throughout the experimental duration. Special thanks for technicians for their efforts to finalize the experiment precisely.

Disclosure statement

No potential conflict of interest was reported by the author(s).

ORCID

Al Sayed Ibrahim Diwedar http://orcid.org/0000-0001-5380-051X

References

Abdelhaleem, F.S., and S, I.A. 2023. "Scour bed morphology caused by partially free and submerged flow at pipe culvert." *J. Hydraul. Eng.*, May. 1–15. doi:10.1080/09715010.2023.2211038.

Abdulabbas, F., Khassaf, S.I., and Omran, H.A. 2015. "The Effect of relative discharge on local scour downstream combined structure." *Inter. J. Sci. Eng. Res*, 6(10), October. ISSN 2229–55.

Abozeid, G., Waeel, E., Mohamed, W.E., and Osman, N.M.E. 2019. "Experimental study on bed scour and its protection behind standing wave weirs considering combined flow over weir crested bottom pipes." *JES. Journal Of Engineering Sciences*, 47(4), July. 461–474. doi:10.21608/JESAUN.2019.115495.

Alhealy, M.K.M., and Hayawi, G.A.A.M. 2019. "Experimental study of the scour depth at downstream weirs has different holes." *Al-Rafidain Engineering Journal (AREJ)*, 24(1), 18–23. doi:10.33899/rengj.2019.163111.

Ali, A.M., Ibrahim, M., and I, D.A. 2015. "The discharge coefficient for a compound sharp crested V notch weir." *Asian J. Eng. Technol.*, 3 (5), 494–501.

Basiouny, M.E., Nasrallah, T.H., Abdelhaleem, F.S., and Ibraheem, A.S. (2018a), "Roughened and corrugated aprons as scour countermerrged hydraulic jumps", Twenty-first International Water Technology Conference, IWTC21, Ismailia, 28-30 June 2018, 200–214.

Basiouny, M.E., Nasrallah, T.H., Abdelhaleem, F.S., and Ibraheem, A.S. 2018b. "Use corrugated beds to improvement downstream local scour characteristics." *Inter. J. Sci. Eng. Res*, 9(7), 172–176.

Daneshfaraz, R., Minaei, O., Abraham, J., Dadashi, S., and Ghaderi, A. 2019. "3-D numerical simulation of water flow over a broad-crested

weir with openings." *ISH J. Hydraul. Eng.*, 1–9. doi:10.1080/09715010.2019.1581098. 27(sup1).

Dehghani, A.A., Bashiri, H., and Dehghani, N. 2010. "Downstream scour of combined flow over weirs and below gates." In A. Dittrich, K. Koll, J. Aberle, and P. Geisenhainer. (Eds) *(Hg.): River flow 2010*, Karlsruhe: Bundesanstalt für Wasserbaupp. S. 1201–1206.

Dey, S., and Barbhuiya, A.K. 2005. "Time variation of scour atabutments." *J. Hydraul. Eng.*, 131(1), 11–23. doi:10.1061/(ASCE)0733-9429(2005)131:1(11).

Dey, S., Raikar, R.V., and Roy, A. 2008. "Scour at submerged cylindrical obstacles under steady flow." *J. Hydraul. Eng.*, 134(1), 105–109. doi:10.1061/(ASCE)0733-9429(2008)134:1(105).

Elkiki, M. 2018. "Estimation of scour depth downstream the skew V-notch weirs using artificial neural network and gene expression program." *International Water Technology Journal*, 8(1), 1–14.

El-Mahdy, M. E. 2021. "Experimental method to predict scour characteristics downstream of stepped spillway equipped with V-Notch end sill." *Alex. Eng. J.*, 60(5). October. 4337–4346. doi:10.1016/j.aej.2021.03.018.

Googheri, Y.S., Saneie, M., and Ershadi, S. 2017. "Three-dimension numerical simulation of scour temporal changes due to flow in the downstream of combined weirs and gate model." *Civ. Eng. J*, 3(11), 1111. doi:10.28991/CEJ-030941.

Hamed, Y.A., El-Kiki, M.H., and Mirdan, A.M. (2009). "Scour downstream oblique V-notch weir", in: Thirteenth International Water Technology Conference, IWTC 13, Hurghada, Egypt, pp. 853–872.

Helal, E.Y. 2014. "Minimizing scour downstream of hydraulic structures using single line of floor water jets." *Ain Shams Eng. J., ASEJ*, 5 (1). 17–28. doi:10.1016/j.asej.2013.06.001.

Ibrahim, M.M. 2015. "Bed profile downstream compound sharp crested V-notch weir." *Alex. Eng. J.*, 54(3). 607–613. doi:10.1016/j.aej.2015.03.026.

Ibrahim, A., Nasrallah, T.H., Abdelhaleem, F.S., and Basiouny, M.E. 2018. "Influence of gravel beds on erosion of sand by submerged jets." *Saudi J. Civ. Eng*, 2(1), Jul-Aug. 45–50.

Latifi, A., Hosseini, S.A., and Saneie, M. 2018. "Comparison of downstream scour of single and combined free-fall jets in co-axial and non-axial modes." *Model. Earth Syst. Environ.*, 4(3), 1271–1284. doi:10.1007/s40808-018-0501-6.

Martínez, J., Reca, J., Morillas, M.T., and López, J.G. 2005. "Design and calibration of a compound Sharp-Crested Weir." *J. Hydraul. Eng.*, 131(2). doi:10.1061/(ASCE)0733-9429. 112–116.

Melville, B.W. and Chiew, Y.M.1999. "Time scale for local scour at bridge piers." *J. Hydraul. Eng.*, 125(1). 59–65. doi:10.1061/(ASCE)07339429(1999)125:1(59).

Mohamed, I.M., and Abdelhaleem, F.S. 2020. "Flow downstream sluice gate with orifice." *Ksce J. Civ. Eng.*, 24(12). 3692–3702. doi:10.1007/s12205-020-0441-3.

Namadian, B., and Asadi, E. 2022. "Investigation of temporal variations of scour depth in combined weir-gate structure using FLOW-3D numerical model." *Iranian Journal Of Irrigation & Drainage*, 16(2). 432–445.

Ogden, F.L., Crouch, T.D., Pradhan, N.R., and Kempema, E. 2011. "Laboratory investigation of sedimentation effects on V-Notch weirs." *World Environmental And Water Resources Congress*. doi:10.1061/41173(414)500.

Omran, H.A., Khassaf, S.I., and Hassan, F.A. 2016. "The effect of flow conditions and geometric parameters on the scour value downstream composite structures of Weir and gate." *Kufa J. Eng.*, 7(1), January. 115–128. doi:10.30572/2018/KJE/711217.

Rezazadeh, H., Manafpour, M., and Ebrahimnezhadian, H. 2020. "Three-dimensional simulation of flow over sharp-crested weirs using volume of fluid method." *Journal Of Applied Engineering Sciences*, 10(1), 75–82. doi:10.2478/jaes-2020-0012.

Saadatnejadgharahassanlou, H., Zeynali, R.I., Gharehbaghi, A., Mehdizadeh, S., and Vaheddoost, B. 2019. "Three-dimensional flow simulation over a sharp-crested V-Notch weir." *Flow Meas. Instrum.*, 101684 doi:10.1016/j.flowmeasinst.2019.101684. 101684.

Saad, N.Y., and Fattouh, E.M. 2016. "Hydraulic characteristics of flow over weirs with circular openings." *Ain Shams Eng. J.*, 8(4), December. 2017. 515–522. doi:10.1016/j.asej.2016.05.007.

Shan, H., Zhaoding Xie, C.B., Suaznabar, O., Steven Lottes, J.S., and Kerenyi, K. 2012. *Submerged flow bridge scour under clear water conditions*, Publication No. FHWA-HRT-12-034. Washington, DC, Federal Highway Administration.

Sheppard, D.M., Melville, B., and Demir, H. 2013. "Evaluation of existing equations for local scour at bridge piers." *J.Hydraul. Eng.*, 140(1), 14–23. doi:10.1061/(ASCE)HY.1943-7900.0000800.

Tanimu, B., Be, B.A., Muhammad, M.M., and Wada, S.A. 2021. "Experimental study of flow through trapezoidal weir Controlled under a semi-circular gate." *FJS*, 5(2), 145–154. doi:10.33003/fjs-2021-0502-634.

Trishan, B. (2020): "Basis of soil classification" soilmanagementindia. com/soil/soil-classification/basis-of-soil- classification/13460, visited on: 4/1/2020. (16) (PDF) impact of bed material on the local scour downstream Fayoum type weir with various designs of floor jets. [accessed Nov 16 2021]. https://www.researchgate.net/publication/339527743_Impact_of_Bed_Material_on_the_Local_Scour_Downstream_Fayoum_Type_Weir_with_Various_Designs_of_Floor_Jets

Zhang, H., Nakagawa, H., Kawaike, K., and Yasuyuki, B.A.B.A. 2009. "Experiment and simulation of turbulent flow in local scour around a spur dyke." *Int. J. Sediment Res*, 24(1). 33–45. doi:10.1016/S1001-6279(09)60014-7.